

## Supporting Information

# Glucose Oxidase-Instructed Traceable Self-Oxygenation/Hyperthermia Dually Enhanced Cancer Starvation Therapy

Ting He<sup>a,b,†</sup>, Han Xu<sup>a,†</sup>, Yifan Zhang,<sup>a</sup> Shijian Yi,<sup>c</sup> Run Cui,<sup>a</sup> Shaojun Xing,<sup>a</sup> Chaoliang Wei,<sup>a</sup>  
Jing Lin,<sup>a</sup> Peng Huang<sup>a,\*</sup>

<sup>a</sup> Marshall Laboratory of Biomedical Engineering, International Cancer Center, Laboratory of Evolutionary Theranostics (LET), School of Biomedical Engineering, Shenzhen University Health Science Center, Shenzhen 518060, China

<sup>b</sup> Key Laboratory of Optoelectronic Devices and Systems of Ministry of Education and Guangdong Province, College of Optoelectronic Engineering, Shenzhen University, Shenzhen 518060, China

<sup>c</sup> Department of General Surgery, Shenzhen University General Hospital, Shenzhen 518055, China

### Corresponding author:

Peng Huang

**Addresses:** 1066 Xueyuan Boulevard Shenzhen University Health Science Center, Shenzhen, 518060, China. E-mail: [peng.huang@szu.edu.cn](mailto:peng.huang@szu.edu.cn) (Peng Huang)

† These authors contributed equally to this work.

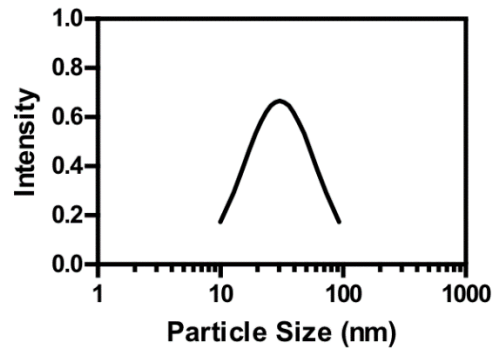


Figure S1 Particle size distribution of MNS.

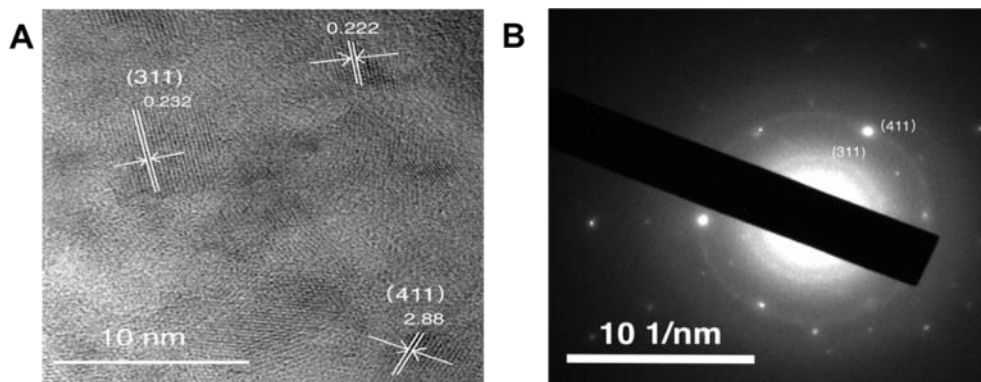


Figure S2 HRTEM images (A) and SAED pattern (B) of MNS .

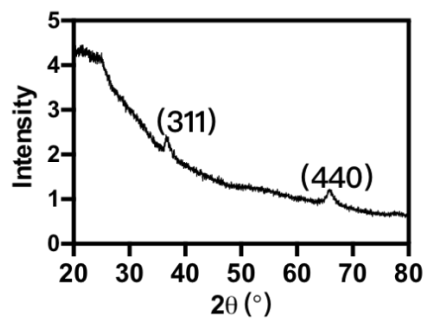
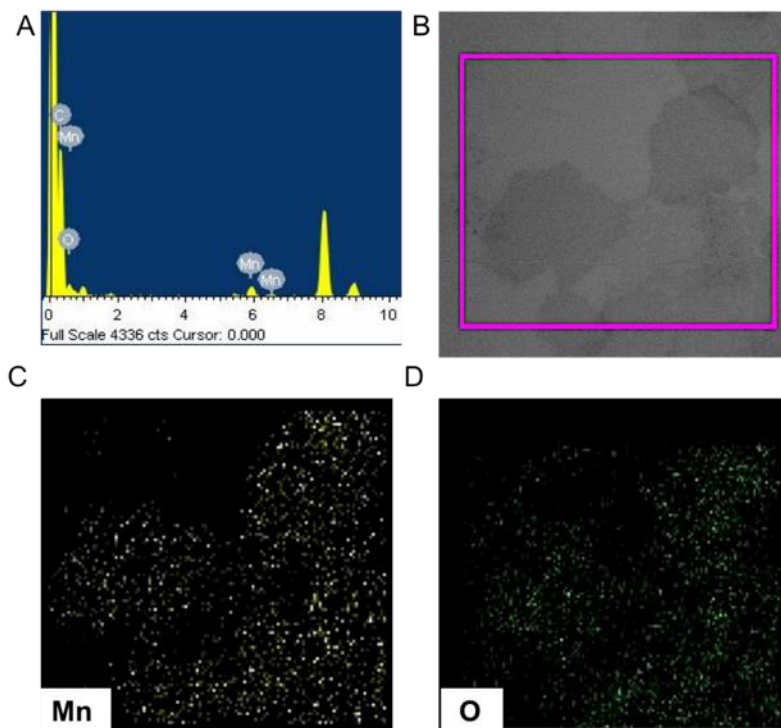
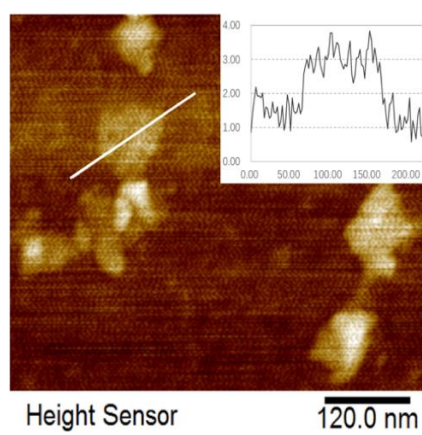


Figure S3 XRD pattern of MNS (JCPDS Card 80-1089).



**Figure S4** (A) EDX spectra of MNS. EDX elemental mapping of MNS (B) and the corresponding elements: Mn (C), O (D).



**Figure S5** AFM image and its thickness of MNS.

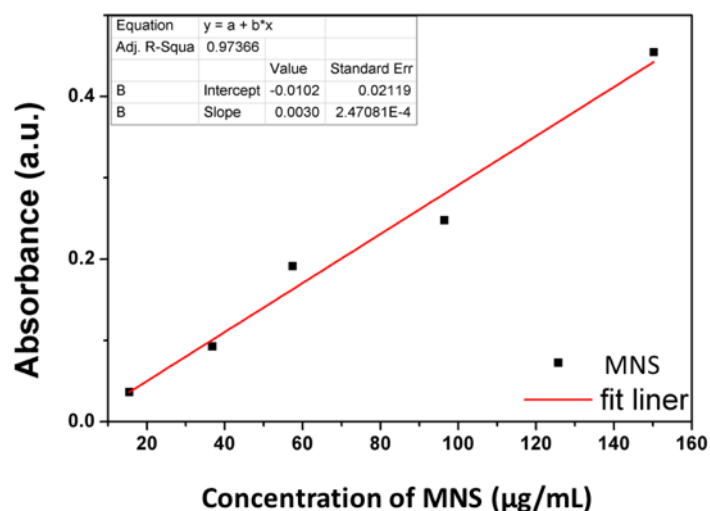


**Figure S6** Optical density (OD) of MNS at 808 nm as a function of concentration, described by

$$Y=0.003X-0.0102 \quad (R^2=0.9736)$$

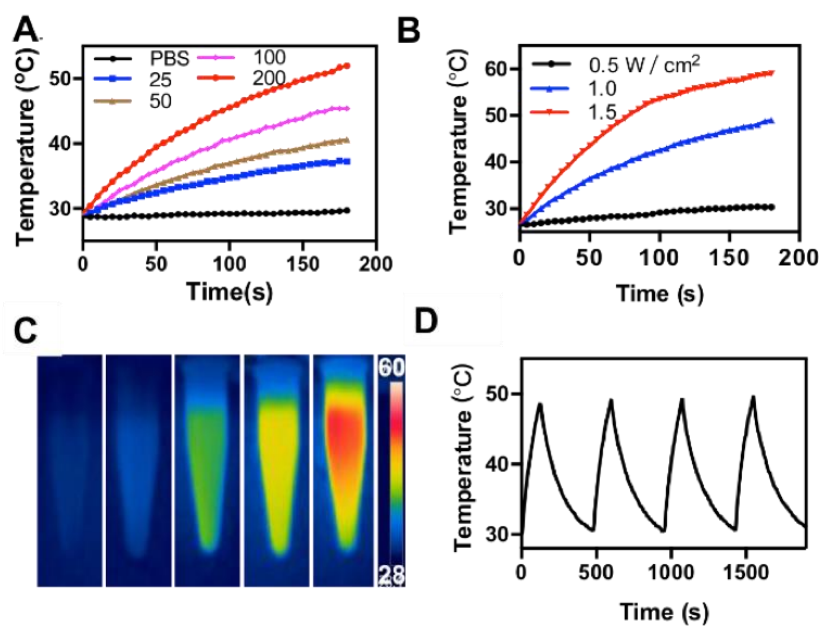


**Figure S7** (A) The 808 nm laser-induced heat generation of PBS, 25, 50, 100, 200  $\mu\text{g/mL}$  MNS aqueous solution with laser power density of 1  $\text{W/cm}^2$ . (B) The temperature of 200  $\mu\text{g/mL}$  MNS solution irradiated with 0.5, 1, 1.5  $\text{W/cm}^2$  808 nm laser. (C) Thermal images of PBS, 25, 50, 100, 200  $\mu\text{g/mL}$  MNS after 3 min exposed to 1  $\text{W/cm}^2$  808 nm laser. (D) The temperature of 200  $\mu\text{g/mL}$  MNS solution irradiated by an 808 nm laser (1  $\text{W/cm}^2$ ) for four on/off cycles (on: 2 min, off: 6 min).

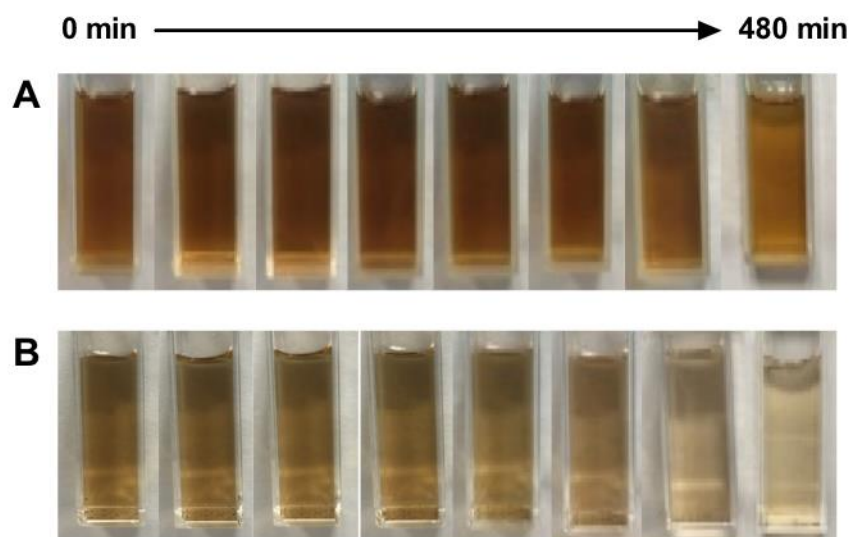


**Figure S8** Digital photos of MNS (A) and MNS-GOx (B) in 5 mM glucose PBS pH=7.4

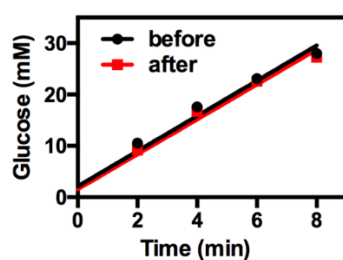


**Figure S9** Glucose reaction rate of MNS-GOx before and after 808 nm laser ( $1 \text{ W/cm}^2$ , 5 min) irradiation at  $30^\circ\text{C}$ .

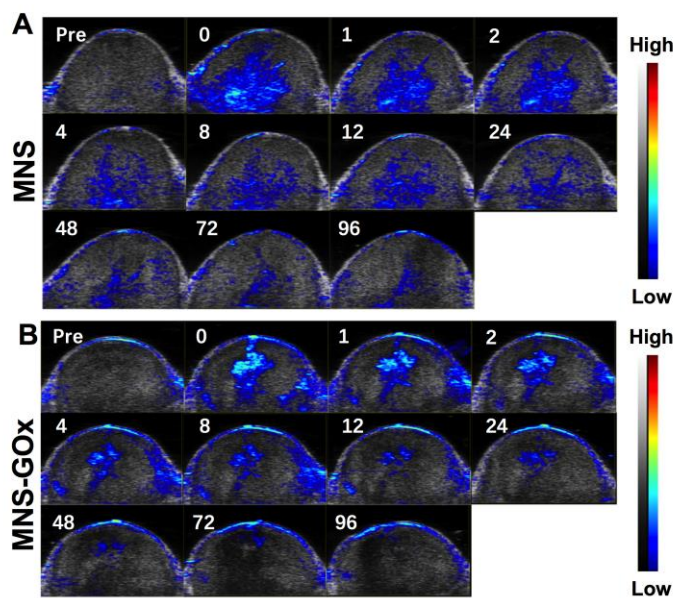


**Figure S10** PA images of mice treated with MNS and MNS-GOx, the images were recorded at 0, 1, 2, 4, 8, 12, 24, 48, 72, 96 h.

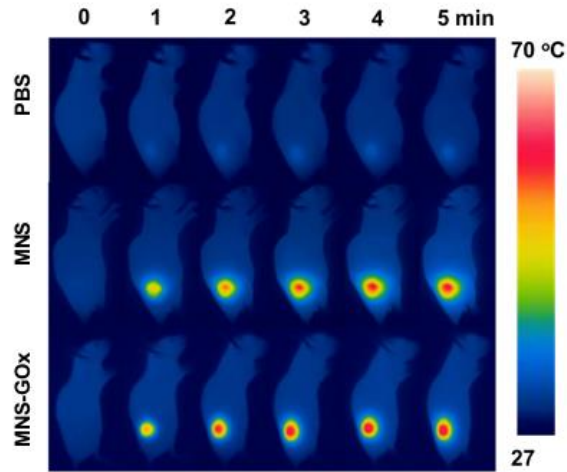


**Figure S11** Thermal images of tumor irradiation by an 808 nm laser (1 W/cm<sup>2</sup>) after different treatments at a series of time points.

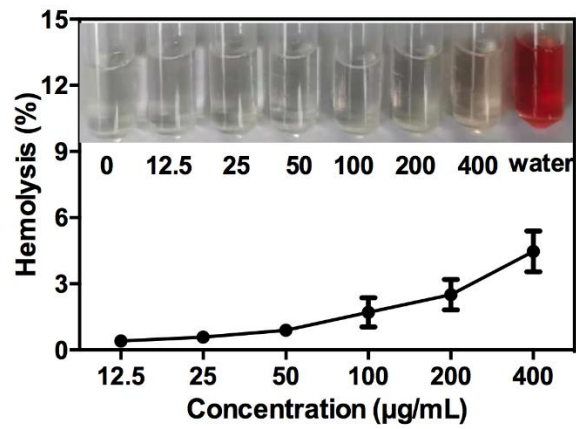


**Figure S12** Hemolysis analysis of MNS solution at various concentrations. The mixtures were centrifuged after kept standing for 4 h, then the absorbance of supernatant was measured to detect the hemoglobin.

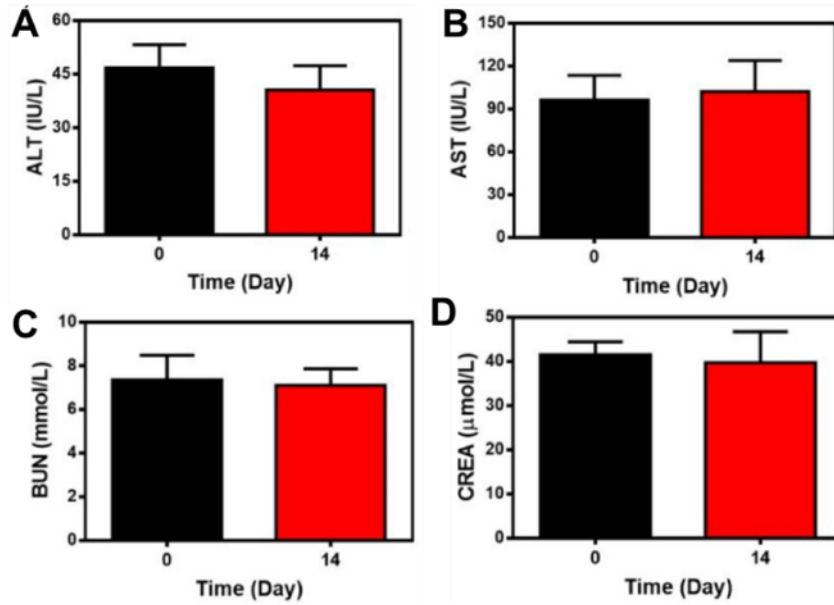


**Figure S13** Blood biochemistry results of nude mice before (0 day) and after (14 day) injection of MNS-GOx: ALT (A), AST (B), BUN (C) and CREA (D).

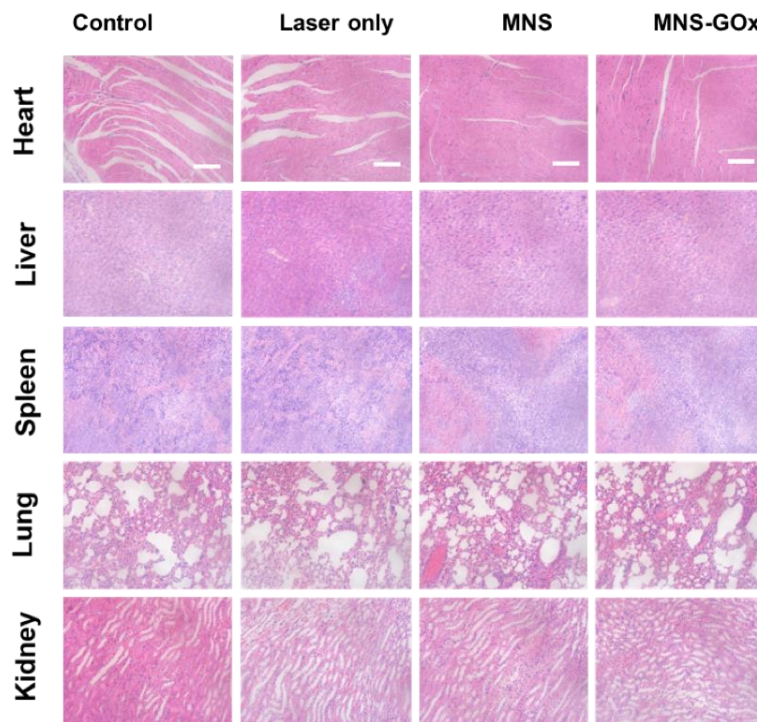


**Figure S14** H&E staining images of main organs after 30 d of treatment with different treatments.

Scale bar: 100  $\mu$ m.